

Schell, Juliana; Schaaf, Peter; Vetter, Ulrich; Lupascu, Doru C.:

TDPAC study of Fe-implanted titanium dioxide thin films

Original published in: AIP Advances. - New York, NY : American Inst. of Physics. - 7 (2017), 9, art. 95010, 7 pp.
Original published: 2017-09-12
ISSN: 2158-3226
DOI: [10.1063/1.4994247](https://doi.org/10.1063/1.4994247)
[Visited: 2019-03-26]



This work is licensed under a [Creative Commons Attribution 4.0 International license](https://creativecommons.org/licenses/by/4.0/). To view a copy of this license, visit <http://creativecommons.org/licenses/by/4.0/>

TDPAC study of Fe-implanted titanium dioxide thin films

Juliana Schell,^{1,2,a} Peter Schaaf,³ Ulrich Vetter,³ and Doru C. Lupascu²

¹European Organization for Nuclear Research (CERN), CH-1211 Geneva, Switzerland

²Institute for Materials Science and Center for Nanointegration, Duisburg-Essen (CENIDE), University of Duisburg-Essen, 45141 Essen, Germany

³Department of Materials for Electronics, Technical University of Ilmenau, Gustav-Kirchhoff-Straße 5, 98693 Ilmenau, Germany

(Received 5 July 2017; accepted 5 September 2017; published online 12 September 2017)

Fe-doping in TiO₂ has been proven to improve several of its properties, including the photocatalytic activity. Time-differential perturbed angular correlation (TDPAC) as the applied spectroscopy method is particularly interesting because it can probe the electric and magnetic interactions on a local atomic scale. In this work the hyperfine interactions on ¹¹¹Cd atoms substituting Ti atoms in TiO₂ due to nearby Fe atoms also diluted within the TiO₂ lattice were measured as a function of temperature. The results review two fractions with distinct quadrupole interaction parameters. One site, occupied by the ¹¹¹Cd probes, presents the smaller quadrupole interaction frequency, namely $\nu_{q1} = 45$ MHz, and can be ascribed to sites that are more distant from the Fe substitutional site whereas the second site characterized with $\nu_{q2} = 62$ MHz is related to Cd probe atoms that are closer to the Fe defect. Additionally, the system has been characterized using electron dispersive spectroscopy. © 2017 Author(s). All article content, except where otherwise noted, is licensed under a Creative Commons Attribution (CC BY) license (<http://creativecommons.org/licenses/by/4.0/>). [<http://dx.doi.org/10.1063/1.4994247>]

INTRODUCTION

Pure or Fe-doped TiO₂ can be used as photocatalyst for water purification or energy converter in solar cells, besides technology applications in the electronics industry.¹⁻⁴ Furthermore, Fe doping has been proven to improve the photocatalytic activity of titanium oxide and makes possible the absorption of light at a higher wavelength.¹

The TiO₂ was one of the first material to being investigated as diluted magnetic semiconductor (DMS) and ferromagnetism was first reported by Matsumoto et al⁵ in a study done by the addition of Co in the system. The origin of the ferromagnetic coupling is still unknown and is being studied diligently in recent years, and many times this ferromagnetism was associated with the presence of clusters of Co ($T_C \approx 1180$ K).⁶

Following the earliest publication of the work of Dietl et al⁷ several studies have been published investigating the candidates for DMS through measurements and first-principles calculations; one of the most frequent observations was an interaction that would be responsible for magnetism, whose range is determined by the polaron and works for low concentrations of TM associated to oxygen vacancies.

TIME-DIFFERENTIAL PERTURBED ANGULAR CORRELATION OF γ RAYS

The charge distribution at the ¹¹¹In(¹¹¹Cd) induces an electric field gradient (EFG), which modulates the half-life histogram of the intermediate state (84.5 ns). Due to suitable nuclear properties and relative long half-life of the probe, it's possible to follow the evolution of phase transitions as a function of temperature with high sensitivity. The TDPAC technique measures the perturbation

^ajuliana.schell@cern.ch

function $R(t) \approx A_{22}G_{22}(t)$ for different perturbation factors $G_{22}(t)$, as shown in Equation 1, valid for spin 5/2.

$$G_{22}(t) = \sum_{n=0}^3 s_n(\eta) \cos(\omega_n t). \quad (1)$$

The observable ω_n frequencies are given by $\omega_n = 6\omega_Q C_n(\eta)$ respectively. The coefficient C_n can be numerically calculated for a known η .⁸ The coefficients s_n denote the amplitudes of the transition frequencies ω_n and are summations of Wigner 3j-symbols products running over the allowed magnetic splitting hyperfine states.⁹ If there are probe atoms exposed to j different lattice environments, and each of them creates a characteristic field gradient at fraction f of probe atom sites, the perturbation function becomes $R(t) = A_{22} \sum_j f_j G_{22}^j(t)$.

The axial asymmetry of the EFG tensor or deviations from it are described by the asymmetry parameter $\eta = (V_{xx} - V_{yy})/V_{zz}$. The major component of the EFG tensor V_{zz} can be obtained from quadrupole frequency ν_Q by:

$$\nu_Q = \frac{eQV_{zz}}{h}, \quad (2)$$

with Q being the nuclear quadrupole moment. Additional details about the TDPAC technique can be found in Refs. 8–10.

In the present work we measured the signal that can be obtained from the hyperfine interactions by means of time-differential perturbed angular correlation (TDPAC) on Cd probe atoms inserted into Fe-doped TiO₂. One envisaged advantage of such a study is that potentially one can get information about electric and magnetic interactions on an atomic scale without the need of application of an external magnetic and as a function of temperature.

EXPERIMENTAL

The TiO₂ samples were prepared as thin films. It was sputter deposited onto a Si(100) substrate. The thickness of the film was 100 nm. During the deposition the temperature of the substrate was kept at 363 K. The atmosphere was composed of Ar and O₂ gases and the target was composed of Ti with a purity of 99,999% and 3% of Fe was ion implanted at room temperature using the ion implanter Bonn Separator (BONIS)^{11,12} at the University of Bonn. An introduction to the implantation methodologies can be found in the reference 4.

The BONIS facility allows to implant a wide variety of ions (stable or radioactive). Furthermore, by varying its implantation energy, it is possible to investigate material properties from the surface to depths of several tens of nanometers. The Fe was ion implanted at 80 keV with a dose of 10¹⁵ atoms/cm². The second implantation was performed at 160 keV using ¹¹¹In. The hyperfine interactions measurements were recorded using a TDPAC spectrometer equipped with 4 BaF₂ detectors. The first measurement was made at room temperature with the as implanted sample. Subsequent measurements were performed increasing the measurement temperature of the sample to 473 K, 573 K, 623 K, 673 K, 44 K, 100 K, 150 K and 200 K with the help of a furnace made of graphite resistance and a cryostat system. After that, rapid thermal annealing (RTA) at 873 K for 10 min in vacuum was performed. Then, the last measurement was performed at room temperature. All TDPAC spectra were taken in the Raghavan geometry inside a TDPAC furnace.¹³ Since the theoretical anisotropic coefficients of nuclear decay apply only to point-shaped detectors, their values were corrected according to the geometry of the BaF₂ detectors of the setup used.¹⁴ The attenuation coefficients can be numerically calculated according to reference 15 and the anisotropy coefficients were determined by Monte Carlo simulations. Moreover, the obtained spectra were fitted with a multiplicative constant using the calculated anisotropy coefficients. Finally, from this constant and the assumed anisotropy coefficients, the effective anisotropic coefficients could then be calculated. Theoretical perturbation functions were fitted to the spectra using the Nightmare¹⁶ software to extract the hyperfine parameters.

RESULTS AND DISCUSSION

The results of the TDPAC experiments are shown in the Figures 1 and 2. The hyperfine parameters obtained from fits of the experimental perturbed angular correlation anisotropy functions $R(t)$ are given in Table I and Figure 3.

Two cadmium probe sites with distinct electric hyperfine interaction parameters were necessary in order to obtain satisfactory fit to the data. Just after the ion implantation, at 295 K, the $R(t)$ TDPAC curve can be fitted to two anisotropy functions with very similar quadrupole frequencies $\nu_q = 70$ MHz but with different asymmetry parameters, namely, $\eta_1 = 0.14$ and $\eta_2 = 0.70$. The second site presents large width of the frequencies distribution $\delta_2 = 28\%$. This feature is assigned to a large distribution of different sites originated from local defects caused by the process of ion implantation.

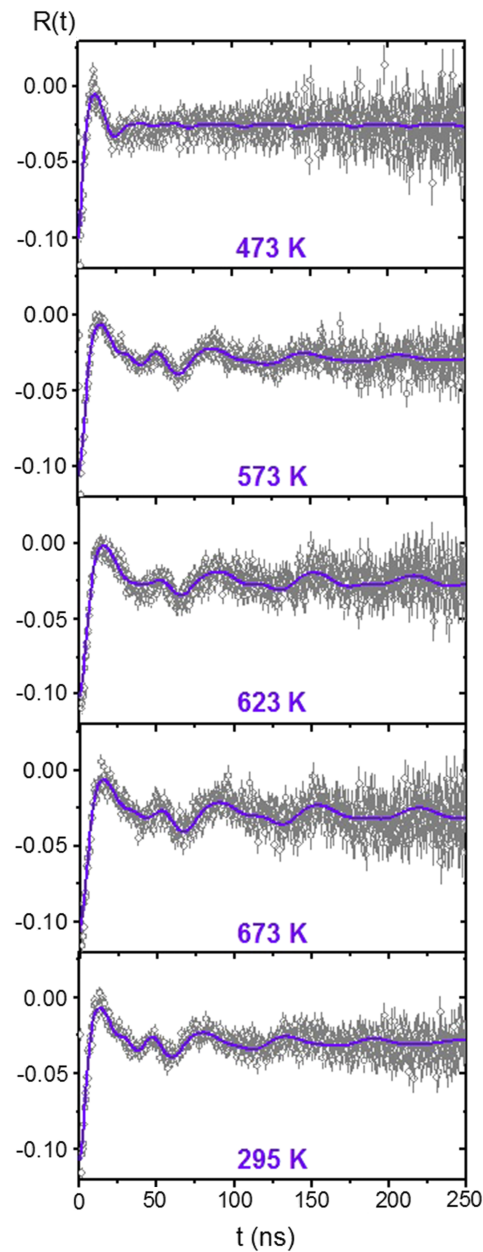


FIG. 1. TDPAC spectra of $^{111}\text{In}(^{111}\text{Cd})$ probes implanted into Fe-doped TiO_2 . The least-squares fits of the hyperfine parameters are represented by the solid curves. The order of the spectra corresponds to the measurement sequence.

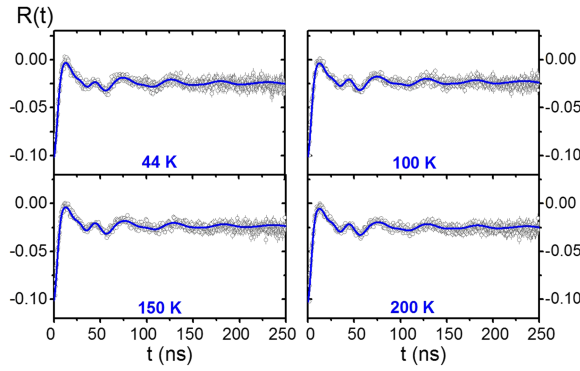


FIG. 2. TDPAC spectra of $^{111}\text{In}(^{111}\text{Cd})$ probes implanted into Fe-doped TiO_2 measured below room temperature. The least-squares fits of the hyperfine parameters are represented by the solid curves.

After a rapid thermal annealing at 873 K no quadrupole interactions were observed because the Cd probes migrated out of the sample. In view of the behaviour mentioned above, it can be concluded that the Fe-doped TiO_2 can be characterized by assuming two distinct sites for In-Cd occupation. The frequency distribution widths are $\delta_1 = 6\%$ and $\delta_2 = 21\%$ and the respective fraction of sites are $f_1 = 32\%$ and $f_2 = 68\%$. Magnetic hyperfine interactions were not detected. If existing they are too weak and are masked by the relatively large distribution of the EFG's.

The electronic structure of pure TiO_2 consists of a valence band formed by hybrid $\text{Ti}^{3d}\text{-O}^{2p}$ wave functions with predominance of the oxygen 2p states. The same hybrids form the conduction band but in this case the predominance is for the Ti^{3d} states. When an impurity atom such as Fe substitutes for a Ti atom, it transfers part of its 3d electrons to the valence band hybrids as well as it forms localized states at the band gap between the valence and conduction band, repositioning the Fermi level of the defect compound relative to the pure TiO_2 compound. The more affected atoms are those that are neighbours of the foreign atom defect. As a result, the neighbouring atoms around a Fe atom substituting for Ti in TiO_2 becomes spin-polarized due to the super-exchange mechanism. One of the ways this spin-polarization can be seen locally is by means of the transferred magnetic hyperfine fields.

The magnetic interactions between atoms in Fe-doped TiO_2 are mediated by the super-exchange mechanism. The spin-polarizations exchanged by the transition elements are mediated by oxygen atoms. There are two different paths that link two Ti atoms in TiO_2 that differ in the angle formed by the respective Ti-O-Ti bond, as shown in Figure 4. Moreover, high magnetization has been observed in sub-nanostructured Fe_3O_4 film by a phenomenon called spin-flipping of the valence-spin tetrahedral Fe^{3+} .¹⁷ However, a secondary phase hasn't been observed in our work.

Figure 5 shows complementary electron dispersive spectroscopy analysis of the thin films on the substrate with no indication of Fe presence in the indicated analyzed region. The analysis has been

TABLE I. Electric field gradient parameters (EFG) resulting from fits on TDPAC spectra resulted from experiments at several temperatures and experimental conditions. The TDPAC data were fitted by assuming two distinct sites for Cd probes labelled site 1 and 2. EFG frequencies ν_q in MHz, Gaussian distribution of frequencies δ and fraction of sites f given in %. η is the asymmetry parameter of the EFG.

T (K)	ν_{q1}	η_1	δ_1	f_1	ν_{q2}	η_2	δ_2	f_2
44	82(5)	0.28(2)	8.2(4)	31(3)	54(4)	0.42(3)	21(2)	69(5)
100	82.2(5)	0.28(2)	7.5(4)	26(2)	54(4)	0.39(3)	23(2)	74(5)
150	83(5)	0.26(2)	8.2(4)	27(3)	53(4)	0.36(3)	21(2)	73(4)
200	84(5)	0.27(2)	7.9(4)	26(3)	53(4)	0.36(3)	22(2)	74(4)
295	77(4)	0.14(1)	5.0(3)	6.0(5)	78(4)	0.70(2)	28(1)	94(4)
473	85(5)	0.00	1.1(2)	3.0(3)	69(5)	1.00(4)	33(3)	97(3)
573	48(3)	0.24(2)	8.0(4)	31(2)	70(4)	0.44(3)	17(1)	69(4)
623	46(2)	0.28(2)	5.0(4)	27(2)	62(3)	0.54(5)	22(1)	73(3)
673	45(3)	0.25(2)	6.0(5)	32(3)	58(4)	0.48(3)	21(2)	68(5)

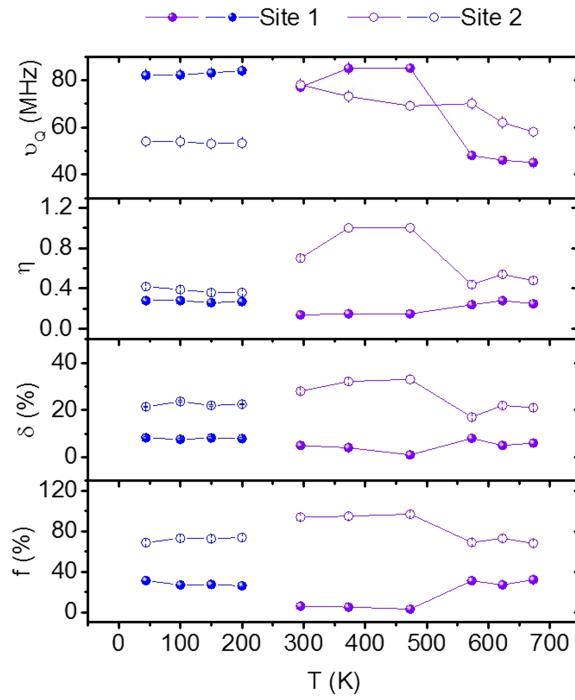


FIG. 3. Hyperfine parameters and their respective errors in the Fe-doped TiO_2 thin film using ^{111}In (^{111}Cd) as the test nucleus. Some error bars cannot be seen, because their uncertainties are smaller than the data points.

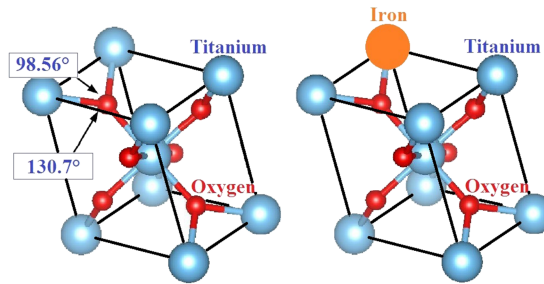


FIG. 4. Unitary TiO_2 cells where it is shown the two different angles of the Ti-O-Ti bonds (a) and for Fe replacing the Ti-site with a Ti-O-Fe bond with the smallest angle (b).

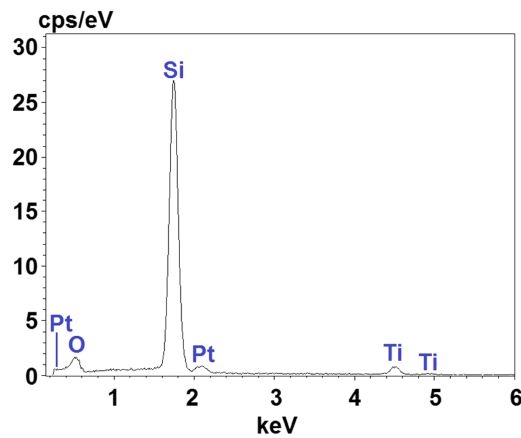


FIG. 5. Electron dispersive spectroscopy (EDS) analysis of the thin film in rutile phase.

performed after the decay of the probe nuclei. The Pt cover was used for increasing conduction for the scanning electron microscopy method. Since the analysis has been performed without removing the Si substrate, the amount of 3 % of Fe was under the detection limit of the technique.

The origin of the ferromagnetism in Fe-implanted TiO₂ is an open question and has been also assigned to α -Fe nanoparticles.¹⁸ The implantation process can induce the formation of small precipitates of FeTi₂O₅¹⁹ and Fe₃O₄ phases.²⁰ The presence of Fe³⁺ and Fe²⁺ was studied as a function of annealing temperature by emission Mössbauer spectroscopy²¹ at ISOLDE-CERN,²² in which Fe³⁺ was found in paramagnetic state.

CONCLUSIONS

It was observed that the TDPAC spectra are composed of two fractions of probe sites with distinct quadrupole interaction parameter sets while from the theoretical point of view one can say that the distribution of possible sites to be occupied by the Cd probes can be separated into two groups. One group of sites occupied by the In-Cd probes is represented by the smaller quadrupole interaction frequency, namely ν_{q1} , which can be ascribed to sites that are more distant from the Fe substitutional site,^{3,4} whereas the second site characterized with ν_{q2} is related to Cd probe atoms that are closer to the Fe defects. Hyperfine interactions of magnetic origin were not detected experimentally. From the theoretical point of view, they exist but their influence on the experimental TDPAC spectra are very small due to two reasons: a) the majority of the sites might sense a very small hyperfine magnetic field, and b) only a small fraction of sites would produce a larger hyperfine magnetic field. This field can easily be masked due to the large distribution of EFG's presented by these samples.

The study shown this work is part of PhD thesis²³ and was presented on a poster section, which took place at the *DPG Spring Meeting of the Condensed Matter Section (SKM)* and was held at the University of Regensburg, Germany, in 2013.

ACKNOWLEDGMENTS

This work has been funded by the Federal Ministry of Education and Research (BMBF) through grants 05K13TSA and 05K16PGA and DAAD/CNPq through grant 290102/2011-1. We thank Ms. Cornelia Noll and the BONIS team at HISKP, Bonn, for the implantations and the warm hospitality. PD. Reiner Vianden and Prof. Dr. Artur Wilson Carbonari are thankfully acknowledged for discussions about the TDPAC technique. We extend our thanks to Prof. Ronaldo Mansano for the production of high quality films.

- ¹ S. H. Othman, S. A. Rashid, T. I. M. Ghazi, and N. Abdullah, *Journal of Nanomaterials* **2011**, 571601 (2011).
- ² M. Cargnello, T. R. Gordon, and C. B. Murray, *Chemical Reviews* **114**, 9319 (2014).
- ³ J. Schell, D. C. Lupascu, J. G. M. Correia, A. W. Carbonari, M. Deicher, M. B. Barbosa, R. D. Mansano, K. Johnston, I. S. Ribeiro, Jr., and ISOLDE collaboration, *Hyperfine Interactions* **238** (2016).
- ⁴ J. Schell, D. C. Lupascu, A. W. Carbonari, R. D. Mansano, I. S. Ribeiro, Jr., T. T. Dang, I. Anusca, H. Trivedi, K. Johnston, and R. Vianden, *Journal of Applied Physics* **121**, 145302 (2017).
- ⁵ Y. Matsumoto, M. Murakami, T. Shono, T. Hasegawa, T. Fukumura, M. Kawasaki, P. Ahmet, T. Chikyow, S.-ya Koshihara, and H. Koinuma, *Science* **291**, 854 (2001).
- ⁶ R. Janisch, P. Gopal, and N. A. Spaldin, *Journal of Physics Condensed Matter* **17**, R657 (2005).
- ⁷ T. Dietl, H. Ohno, F. Matsukura, J. Cibert, and D. Ferrand, *Science* **287**, 1019 (2000).
- ⁸ T. Butz, *Hyperfine Interactions* **52**, 189 (1989).
- ⁹ H. Frauenfelder, R. M. Steffen, and K. Siegbahn, *α -, β - and γ -Ray Spectroscopy*, ed K. Siegbahn (Amsterdam: North-Holland, 1965).
- ¹⁰ A. Abragam and R. V. Pound, *Physical Review* **92**, 943 (1953).
- ¹¹ K. Freitag, *Radiation Effects* **44**, 185 (1979).
- ¹² Group Vianden, Time-differential perturbed angular correlations, Helmholtz-Institut für Strahlen- und Kernphysik (HISKP) (<http://tdpac.hiskp.uni-bonn.de/pac/>). Accessed in July 2017.
- ¹³ M. Arenz, Aufbau und Test eines Hochtemperaturmessofens für γ - γ - Winkelkorrelationsmessungen, Diplomarbeit, Rheinische Friedrich-Wilhelms-Universität Bonn, Germany (1992).
- ¹⁴ H. Koch, Defekt-Fremdatom Wechselwirkung in den hexagonalen Metallen Rhenium und Lutetium, PhD thesis, Rheinische Friedrich-Wilhelms-Universität Bonn, Germany, (1992).
- ¹⁵ M. J. L. Yates, Appendix 9: Finite Solid Angle Corrections, Book: *Alpha-, Beta- and Gamma-ray Spectroscopy*, Edited by K. Siegbahn, vol. 1, 1691 (1965).

- ¹⁶ Nightmare (MDI) Version RC 3 (1.2.0.247). Copyright (2005-2010) from the group Reiner Vianden and (2008-2010) Ronan Nédélec, Bonn University.
- ¹⁷ T. S. Herng, W. Xiao, S. M. Poh, F. He, R. Sutarto, X. Zhu, R. Li, X. Yin, C. Diao, Y. Yang, X. Huang, X. Yu, Y. P. Feng, A. Rusydi, and J. Ding, *Nano Research* **8**, 2935 (2015).
- ¹⁸ G. Talut, H. Reuther, J. Grenzer, and S. Zhou, *Hyperfine Interactions* **191**, 95 (2009).
- ¹⁹ M. Guermazi, G. Marest, A. Perez, B. D. Sawicka, J. A. Sawicki, P. Thenevard, and T. Tyliczszak, *Materials Research Bulletin* **18**, 529 (1983).
- ²⁰ E. N. Dulov, N. G. Ivoilov, D. M. Khripunov, L. R. Tagirov, R. I. Khaibullin, V. F. Valeev, and V. I. Nuzhdin, *Technical Physics Letters* **35**, 483 (2009).
- ²¹ H. P. Gunnlaugsson, R. Mantovan, H. Masenda, T. E. Mølholt, K. Johnston, K. Bharuth-Ram, H. Gislason, G. Langouche, D. Naidoo, S. Olafsson, A. Svane, G. Weyer, and ISOLDE Collaboration, *Journal of Physics D: Applied Physics* **47**, 065501 (2014).
- ²² K. Johnston, J. Schell, J. Correia, M. Deicher, H. Gunnlaugsson, A. Fenta, E. David-Bosne, Â. Costa, and D. C. Lupascu, *Journal of Physics G: Nuclear and Particle Physics, Focus on Exotic Beams at ISOLDE: A Laboratory Portrait*, accepted, 2017.
- ²³ J. Schell, *Investigation of hyperfine parameters in pure and 3d transition metal doped SnO₂ and TiO₂ by means of perturbed gamma-gamma angular correlation spectroscopy* (São Paulo University, Brazil, 2015).